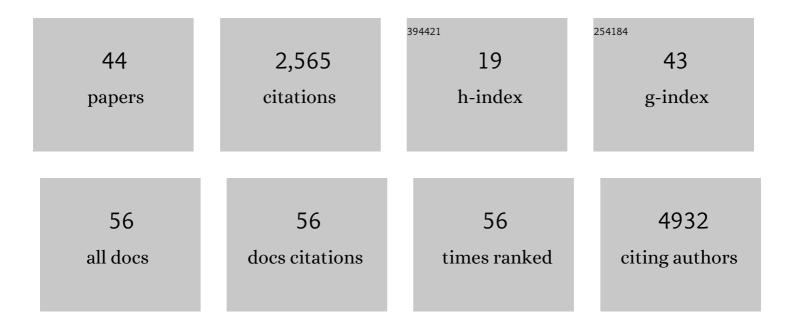
Simon Walker-Samuel

List of Publications by Year in descending order

Source: https://exaly.com/author-pdf/8871179/publications.pdf Version: 2024-02-01



#	Article	IF	CITATIONS
1	Challenges and opportunities of integrating imaging and mathematical modelling to interrogate biological processes. International Journal of Biochemistry and Cell Biology, 2022, 146, 106195.	2.8	5
2	Liver perfusion MRI in a rodent model of cirrhosis: Agreement with bulkâ€flow phaseâ€contrast MRI and noninvasive evaluation of inflammation in chronic liver disease using flowâ€sensitive alternating inversion recovery arterial spin labelling and tissue T1. NMR in Biomedicine, 2021, 34, e4423.	2.8	4
3	Haemodynamic changes in cirrhosis following terlipressin and induction of sepsis—a preclinical study using caval subtraction phase-contrast and cardiac MRI. European Radiology, 2021, 31, 2518-2528.	4.5	3
4	Multifluorescence Highâ€Resolution Episcopic Microscopy for 3D Imaging of Adult Murine Organs. Advanced Photonics Research, 2021, 2, 2100110.	3.6	8
5	Imaging intact human organs with local resolution of cellular structures using hierarchical phase-contrast tomography. Nature Methods, 2021, 18, 1532-1541.	19.0	113
6	Noninvasive diffusion magnetic resonance imaging of brain tumour cell size for the early detection of therapeutic response. Scientific Reports, 2020, 10, 9223.	3.3	29
7	Measuring diffusion exchange across the cell membrane with DEXSY (Diffusion Exchange) Tj ETQq1 1 0.784314	rg₿T/Ove	rloçk 10 Tf 5(
8	Asymmetric Point Spread Function Estimation and Deconvolution for Serial-Sectioning Block-Face Imaging. Communications in Computer and Information Science, 2020, , 235-249.	0.5	5
9	Modelling the transport of fluid through heterogeneous, whole tumours in silico. PLoS Computational Biology, 2019, 15, e1006751.	3.2	35
10	Noninvasive quantification of oxygen saturation in the portal and hepatic veins in healthy mice and those with colorectal liver metastases using QSM MRI. Magnetic Resonance in Medicine, 2019, 81, 2666-2675.	3.0	6
11	Spatiotemporal dynamics and heterogeneity of renal lymphatics in mammalian development and cystic kidney disease. ELife, 2019, 8, .	6.0	46
12	Insights into cerebral haemodynamics and oxygenation utilising in vivo mural cell imaging and mathematical modelling. Scientific Reports, 2018, 8, 1373.	3.3	36
13	Investigating Low-Velocity Fluid Flow in Tumors with Convection-MRI. Cancer Research, 2018, 78, 1859-1872.	0.9	32
14	Computational fluid dynamics with imaging of cleared tissue and of in vivo perfusion predicts drug uptake and treatment responses in tumours. Nature Biomedical Engineering, 2018, 2, 773-787.	22.5	91
15	Non-invasive imaging of disrupted protein homeostasis induced by proteasome inhibitor treatment using chemical exchange saturation transfer MRI. Scientific Reports, 2018, 8, 15068.	3.3	0
16	Studies of copper trafficking in a mouse model of Alzheimer's disease by positron emission tomography: comparison of ⁶⁴ Cu acetate and ⁶⁴ CuGTSM. Metallomics, 2017, 9, 1622-1633.	2.4	20
17	Imaging biomarker roadmap for cancer studies. Nature Reviews Clinical Oncology, 2017, 14, 169-186.	27.6	792
18	Imaging the accumulation and suppression of tau pathology using multiparametric MRI. Neurobiology of Aging, 2016, 39, 184-194.	3.1	42

2

SIMON WALKER-SAMUEL

#	Article	IF	CITATIONS
19	Utilizing confocal laser endomicroscopy for evaluating the adequacy of laparoscopic liver ablation. Lasers in Surgery and Medicine, 2016, 48, 299-310.	2.1	10
20	Use of Caval Subtraction 2D Phase-Contrast MR Imaging to Measure Total Liver and Hepatic Arterial Blood Flow: Preclinical Validation and Initial Clinical Translation. Radiology, 2016, 280, 916-923.	7.3	8
21	Investigating the Vascular Phenotype of Subcutaneously and Orthotopically Propagated PC3 Prostate Cancer Xenografts Using Combined Carbogen Ultrasmall Superparamagnetic Iron Oxide MRI. Topics in Magnetic Resonance Imaging, 2016, 25, 237-243.	1.2	5
22	Acute changes in liver tumour perfusion measured non-invasively with arterial spin labelling. British Journal of Cancer, 2016, 114, 897-904.	6.4	13
23	Monitoring the Growth of an Orthotopic Tumour Xenograft Model: Multi-Modal Imaging Assessment with Benchtop MRI (1T), High-Field MRI (9.4T), Ultrasound and Bioluminescence. PLoS ONE, 2016, 11, e0156162.	2.5	17
24	Decomposition of spontaneous fluctuations in tumour oxygenation using BOLD MRI and independent component analysis. British Journal of Cancer, 2015, 113, 1168-1177.	6.4	15
25	Quantification of light attenuation in optically cleared mouse brains. Journal of Biomedical Optics, 2015, 20, 080503.	2.6	17
26	Gold–silica quantum rattles for multimodal imaging and therapy. Proceedings of the National Academy of Sciences of the United States of America, 2015, 112, 1959-1964.	7.1	107
27	In vivo imaging of tau pathology using multi-parametric quantitative MRI. NeuroImage, 2015, 111, 369-378.	4.2	77
28	Hepatic arterial spin labelling MRI: an initial evaluation in mice. NMR in Biomedicine, 2015, 28, 272-280.	2.8	18
29	Noninvasive Quantification of Solid Tumor Microstructure Using VERDICT MRI. Cancer Research, 2014, 74, 1902-1912.	0.9	185
30	ls Your System Calibrated? MRI Gradient System Calibration for Pre-Clinical, High-Resolution Imaging. PLoS ONE, 2014, 9, e96568.	2.5	26
31	Evaluation and Immunohistochemical Qualification of Carbogen-Induced ΔR2* as a Noninvasive Imaging Biomarker of Improved Tumor Oxygenation. International Journal of Radiation Oncology Biology Physics, 2013, 87, 160-167.	0.8	14
32	In vivo imaging of glucose uptake and metabolism in tumors. Nature Medicine, 2013, 19, 1067-1072.	30.7	427
33	Exploring ΔR ₂ * and ΔR ₁ as imaging biomarkers of tumor oxygenation. Journal of Magnetic Resonance Imaging, 2013, 38, 429-434.	3.4	44
34	A Multi-Parametric Imaging Investigation of the Response of C6 Glioma Xenografts to MLN0518 (Tandutinib) Treatment. PLoS ONE, 2013, 8, e63024.	2.5	10
35	MRI measurements of vessel calibre in tumour xenografts: Comparison with vascular corrosion casting. Microvascular Research, 2012, 84, 323-329.	2.5	16
36	Evaluation of novel combined carbogen USPIO (CUSPIO) imaging biomarkers in assessing the antiangiogenic effects of cediranib (AZD2171) in rat C6 gliomas. International Journal of Cancer, 2012, 131, 1854-1862.	5.1	9

SIMON WALKER-SAMUEL

#	Article	IF	CITATIONS
37	Nonâ€invasive <i>in vivo</i> imaging of vessel calibre in orthotopic prostate tumour xenografts. International Journal of Cancer, 2012, 130, 1284-1293.	5.1	19
38	Extracranial measurements of amide proton transfer using exchangeâ€modulated pointâ€resolved spectroscopy (EXPRESS). NMR in Biomedicine, 2012, 25, 829-834.	2.8	5
39	Improving apparent diffusion coefficient estimates and elucidating tumor heterogeneity using Bayesian adaptive smoothing. Magnetic Resonance in Medicine, 2011, 65, 438-447.	3.0	24
40	Investigating temporal fluctuations in tumor vasculature with combined carbogen and ultrasmall superparamagnetic iron oxide particle (CUSPIO) imaging. Magnetic Resonance in Medicine, 2011, 66, 227-234.	3.0	11
41	Bayesian estimation of changes in transverse relaxation rates. Magnetic Resonance in Medicine, 2010, 64, 914-921.	3.0	28
42	Robust estimation of the apparent diffusion coefficient (ADC) in heterogeneous solid tumors. Magnetic Resonance in Medicine, 2009, 62, 420-429.	3.0	50
43	Evaluation of response to treatment using DCE-MRI: the relationship between initial area under the gadolinium curve (IAUGC) and quantitative pharmacokinetic analysis. Physics in Medicine and Biology, 2006, 51, 3593-3602.	3.0	115
44	The effect of imatinib therapy on tumour cycling hypoxia, tissue oxygenation and vascular reactivity. Wellcome Open Research, 0, 2, 38.	1.8	2